

# LLsM: Generative Linguistic Steganography with Large Language Model

Yihao Wang<sup>†,\*</sup>, Ruiqi Song<sup>†,\*</sup>, Ru Zhang<sup>†,✉</sup>, Jianyi Liu<sup>†</sup>, Lingxiao Li<sup>†,‡</sup>

<sup>†</sup> School of Cyberspace Security, Beijing University of Posts and Telecommunications, China.

<sup>‡</sup> State Key Laboratory of Networking and Switching Technology,  
Beijing University of Posts and Telecommunications, China.

\* These authors are co-first authors.

✉ Corresponding author: zhangru@bupt.edu.cn.

{yh-wang, songrq123, liujy, Lingxiao-Li} @bupt.edu.cn

## Abstract

Linguistic Steganography (LS) tasks aim to generate steganographic text (stego) based on secret information. Only authorized recipients can perceive the existence of secrets in the texts and extract them, thereby preserving privacy. However, the controllability of the stego generated by existing schemes is poor, and the stego is difficult to contain specific discourse characteristics such as style. As a result, the stego is easily detectable, compromising covert communication. To address these problems, this paper proposes **LLsM**, the first LS with the Large Language Model (LLM). We fine-tuned the LLaMA2 with a large-scale constructed dataset encompassing rich discourse characteristics, which enables the fine-tuned LLM to generate texts with specific discourse in a controllable manner. Then the discourse is used as guiding information and inputted into the fine-tuned LLM in the form of the Prompt together with secret. On this basis, the constructed candidate pool will be range encoded and use secret to determine the interval. The same prefix of this interval's beginning and ending is the secret embedded at this moment. Experiments show that LLsM performs superior to prevalent LS-task and related-task baselines regarding text quality, statistical analysis, discourse matching, and anti-steganalysis. In particular, LLsM's MAUVE metric surpasses some baselines by 70%-80%, and its anti-steganalysis performance is 30%-40% higher. Notably, we also present examples of longer stegos generated by LLsM, showing its potential superiority in long LS tasks.

## 1 Introduction

Steganography, a technology for concealing information (Shannon, 1949), embeds secret information within digital media such as texts (Yang et al., 2021)(Yang et al., 2023) and images (Peng et al., 2023)(Luo et al., 2023), obtaining steganographic media that is sensory indistinguishable

from normal media. Steganographic media is transmitted over public channels, and only authorized recipients can perceive whether the media is steganographic and accurately extracts the secret information. Benefiting from the ability of text to be transmitted losslessly over public channels, research on Linguistic Steganography (LS) has explosive growth in recent years (Yang et al., 2021)(Yang et al., 2023)(Huo and Xiao, 2016)(Kim et al., 2010)(Fang et al., 2017)(Yang et al., 2019a)(Zhang et al., 2021)(Zhou et al., 2021)(Lu et al., 2023)(Wang et al., 2023b)(Li et al., 2021). According to the work focuses and embedding ways, LS schemes can be divided into "modified" (Huo and Xiao, 2016)(Kim et al., 2010) and "generative" (Yang et al., 2021)(Yang et al., 2023)(Fang et al., 2017)(Yang et al., 2019a)(Zhang et al., 2021)(Zhou et al., 2021)(Lu et al., 2023)(Wang et al., 2023b)(Li et al., 2021). The focus of the former is to design specific strategies such as synonym replacement (Huo and Xiao, 2016) and syntactic changes (Kim et al., 2010), aiming to embed secret information by modifying the normal carrier (cover). However, the steganographic text (stego) modified by these schemes has poor concealment and is easy to detect by linguistic steganalysis (Yang et al., 2019b)(Yang et al., 2022)(Wang et al., 2023a)(Wang et al., 2023d). In contrast, the latter first employs a language model trained on a corpus to generate high-quality texts. During text generation, a specific encoding way is employed to alter token selection according to the secret information, thereby automatically generating stegos (Fang et al., 2017)(Yang et al., 2019a)(Zhang et al., 2021)(Zhou et al., 2021)(Lu et al., 2023)(Wang et al., 2023b)(Li et al., 2021). These schemes can generate highly concealed stegos that are difficult to perceive and detect.

The concealment of stego determines the success of covert communication to a certain extent. Depending on the constraints, this concealment is

primarily manifested in three aspects: "perceptual", "statistical" and "semantic". "Perceptual concealment" focuses on ensuring that the scheme generates stego with complete and natural sentences. In pursuit of this objective, Fang et al. (Fang et al., 2017) and Yang et al. (Yang et al., 2019a) employed various recurrent neural network architectures to train language models for generating high-quality stegos. The stegos achieved SOTA performance in terms of sentence completeness and naturalness during that period.

"Statistical concealment" requires the statistical distribution of stego to be closely that of the cover. To achieve this goal, Yang et al. (Yang et al., 2021) designed a VAE-Stega scheme with an encoder-decoder architecture. This encoder learns the statistical characteristics of the cover and the decoder generates stego matching these characteristics. These stegos have robust statistical concealment. To further imitate the distribution of cover, Zhang et al. (Zhang et al., 2021) used adaptive dynamic grouping to recursively embed secret information, mathematically proving its robust statistical concealment. Zhou et al. (Zhou et al., 2021) and Lu et al. (Lu et al., 2023) respectively proposed a scheme with generative adversarial networks and a scheme that minimizes perceptual statistical combination distortion. These schemes ensure perceptual and statistical concealment.

"Semantic concealment" aims at generating stego with coherent and specific semantic expressions. To this end, Yang et al. (Yang et al., 2023) utilized semantic information in the encoding and embedding process during translation, maintaining the semantic consistency between cover and stego. Wang et al. (Wang et al., 2023b) improved stego semantic relevance by the relevance of social network context. Li et al. (Li et al., 2021) leveraged knowledge graphs to encode entities and relationships, and this scheme can generate semantically coherent and relevant stegos.

However, these LS schemes still face two primary challenges. On the one hand, if the training data for the language model encompasses distinct types of cover, the content of the generated stegos will be less controllable. On the other hand, these schemes do not consider discourse such as style, genre, and theme, which impacts the effectiveness of concealment at perceptual, statistical, and semantic levels. This results in the generated stegos that lack coherence with certain discourse

characteristics. Eve may perceive the existence of the stegos even without steganalysis techniques, causing covert communication to fail. To overcome these challenges, this paper proposes the **LLsM**, i.e. Large language model-based Linguistic steganography scheme. This scheme fine-tunes the open-source Large Language Model (LLM) LLaMA2 with constructed data that contains rich discourse. The Prompt of the LLM is then directed to generate text consistent with specific discourse characteristics. Based on the secret bitstreams and the range coding of candidate pool, the selection of the subsequent tokens is determined. Repeatedly, LLsM successfully generates stegos that not only exhibit specific discourse characteristics but also effectively conceal secret information.

The main contributions of our work are summarized in the following four points:

- To our knowledge, LLsM is the first work in the LS tasks to use LLM. We use the excellent capable LLaMA2 as the pre-trained language model, and fine-tune LLaMA2 using the constructed dataset with dozens of discourse characteristics, providing a basis for the high-quality stego generation.
- To enhance the semantic concealment of stegos, we analyze the discourse characteristics of the cover such as styles, genres, and themes. These characteristics serve as integral inputs to our steganographic generator, improving the controllability of stego generation.
- To augment the perceptual and statistical concealment of stegos, we use range coding to encode the candidate pool. The interval is determined based on the secret information, and the same prefix matching the beginning and the ending of this interval is the secret embedded at this moment. While guaranteeing strong discourse matching, LLsM better imitates the distribution of cover and ensures the stegos' secure transmission.
- Extensive experiments demonstrate that the LLsM has achieved superior performance in terms of the quality of stego generation, statistical analysis between cover and stego, discourse matching, and anti-steganalysis of stegos. In addition, LLsM can generate long stegos with low perplexity and strong readability, showing its potential advantages in this task.

## 2 LLM Methodology

### 2.1 Modeling

In the "Prisoner Model", in order not to arouse Eve's suspicion and ensure the covert transmission of information, Alice and Bob should enhance the covertness of the stego as much as possible, that is, the distribution  $P_C$  of the cover  $C$  and the distribution  $P_S$  of stego  $S$  should be as close as possible. It can be expressed as:

$$d(P_C, P_S) \leq \varepsilon, \quad (1)$$

where,  $d(\cdot)$  represents the difference measurement method,  $\varepsilon$  is a small value greater than 0, and it measures the concealment of the scheme. Eve's job is to determine whether the transmitted text contains secret information by analyzing whether it conforms to the statistical cover's distribution. However, the limitation of the "Prisoner Model" is that it only considers  $d(P_C, P_S)$  and ignores discourse information of  $S$ , resulting in poor discourse matching between  $C$  and  $S$ .

Affected by distinct user nature and growth environments, social networks are full of texts with various writing styles (Xu et al., 2023a). Furthermore, owing to distinct expression purposes and areas involved, the texts in social networks display different genres (McCarthy and Dore, 2023), such as novels and news. If the steganography scheme ignores discourse information such as the styles, genres, and themes of the texts. At this time, Eve may detect the existence of  $S$  without even analyzing the distribution of the transmitted text, which is incomplete for excellent covert communication.

To ensure a strong discourse matching between  $C$  and  $S$ , Alice and Bob need to ensure that the discourse difference between each transmitted stego and the cover is small enough. Suppose Alice needs to transfer secret information  $m_k \in \mathcal{M}$  to Bob,  $|k|$  is the number of  $m$ . Alice will get the style space  $\mathcal{C}_{style}$  based on the cover  $C$  she writes. According to the specific encoding method  $enc$  and  $m_k$ ,  $S_k$  with the style space  $\mathcal{S}_{style}$  will be generated. To avoid Eve's suspicion of  $S_k$  at the style level, the following conditions need to be satisfied:

$$\begin{cases} f_1 : \text{Stega}(C, enc, m_k) \rightarrow S_k \\ f_2 : C \rightarrow \mathcal{C}_{style} \sim P_{C1}, S_k \rightarrow \mathcal{S}_{style} \\ \quad \quad \quad \sim P_{S1} \\ d(P_{C1}, P_{S1}) \leq \varepsilon_1 \end{cases}, \quad (2)$$

where,  $f_1$  is the steganography process,  $f_2$  is the mapping process from text to style space,  $\text{Stega}(\cdot)$  is the steganography scheme,  $\sim$  is following a certain distribution,  $\varepsilon_1$  is a small value greater than 0, and measures the security at the style level. In addition, if Alice uses a platform that contains a specific genre (such as novels and poems) to publish  $S_k$  that conforms to this genre, Alice will use the platform's genre space  $\mathcal{C}_{genre}$  to generate  $S_k$  with the genre space  $\mathcal{S}_{genre}$ . Or Alice wants to transfer  $m_k$  in the comments on a certain topic and generate  $S_k$  with the theme space  $\mathcal{S}_{theme}$ . To avoid Eve's suspicion of  $S_k$  at the style level and theme level, it needs to be satisfied:

$$\begin{cases} f_3 : C \rightarrow \mathcal{C}_{genre} \sim P_{C2}, S_k \rightarrow \\ \quad \quad \quad \mathcal{S}_{genre} \sim P_{S2} \\ f_4 : C \rightarrow \mathcal{C}_{theme} \sim P_{C3}, S_k \rightarrow \\ \quad \quad \quad \mathcal{S}_{theme} \sim P_{S3} \\ d(P_{C2}, P_{S2}) \leq \varepsilon_2, d(P_{C3}, P_{S3}) \leq \varepsilon_3 \end{cases}, \quad (3)$$

where,  $f_3$  and  $f_4$  are the mapping process of text to style space and theme space,  $\varepsilon_2$  and  $\varepsilon_3$  are smaller values greater than 0, which measure the concealment at the style level and theme level.

The above three assumptions cover most situations where secret information is transmitted over an open channel. Alice and Bob's covert communication hopes to avoid Eve's suspicion to the greatest extent and needs to satisfy:

$$\begin{cases} d(P_C, P_S) \leq \varepsilon \\ (d(P_{C1}, P_{S1}) \leq \varepsilon_1) \vee (d(P_{C2}, P_{S2}) \\ \leq \varepsilon_2) \vee (d(P_{C3}, P_{S3}) \leq \varepsilon_3) \end{cases}. \quad (4)$$

That is, on the premise of ensuring formula 1, excellent covert communication also needs to satisfy at least one discourse-matching condition.

### 2.2 Overall

The LLM proposed in this paper can satisfy the extension of covert communication, i.e. formula 4. LLM not only receives the secret information but also uses the Prompt of LLM (OpenAI, 2023)(Touvron et al., 2023) to input instructions to generate certain discourse characteristics into the LLM as guidance information. This scheme employs range coding to encode the candidate pool, achieving the generated stegos that are both in controlled discourse and highly concealable. Figure 1 shows the overall framework of LLM.

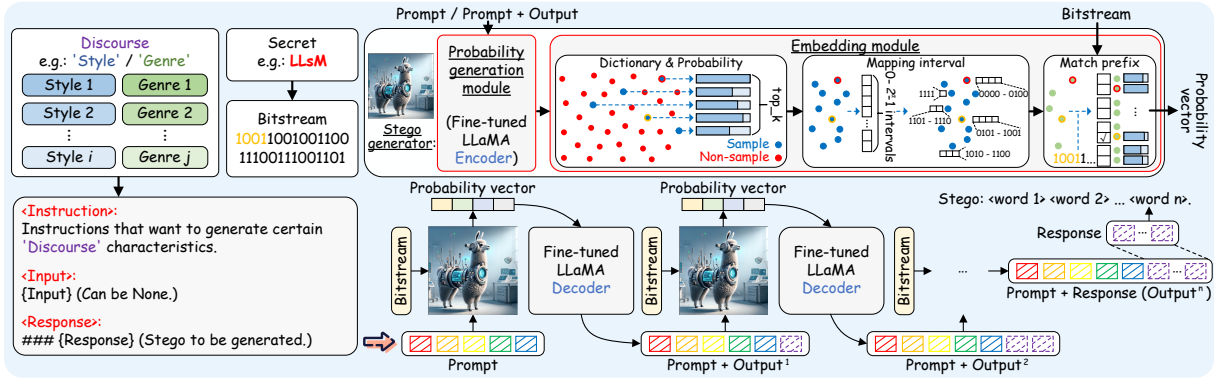


Figure 1: The overall framework of LLMs. The framework mainly consists of two parts: "Probability generation module" and "Embedding module". The input of the "Stego generator" is the secret information bitstream and Prompt containing <Instruction> and <Input>. The output is the generated stegos.

## 2.3 Details

### 2.3.1 LLM Fine-tuning

**Fine-tuning dataset construction.** Figure 2 shows the fine-tuning dataset construction. We used GPT4 (OpenAI, 2023) and Wikipedia<sup>1</sup> to obtain answers, and explored the potential writing habits and genre structures of a certain field contained by humans' writing. These are input into GPT4 (OpenAI, 2023) in the form of Prompt together with the answers for dataset enhancement and expansion. Then high-quality answers are obtained through filtering. These answers are formed golden Q&A with the corresponding questions, and the format of golden Q&A is "Prompt (Instruction, Input), Response".

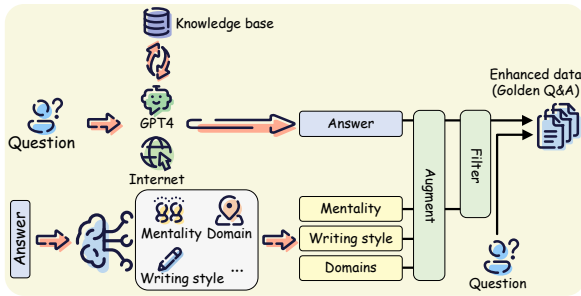


Figure 2: Dataset construction.

**LLaMA2 fine-tuning.** Use the golden Q&A obtained above as input for fine-tuning the LLM. Figure 3 shows the process of LLM fine-tuning. Here, we choose LLaMA2 (Touvron et al., 2023), which is open-sourced by Meta Company, with 2 trillion pre-trained tokens and 4,096 context length. Due to the large scale of this model, direct fine-tuning will bring huge time and space overhead.

<sup>1</sup><https://www.wikipedia.org/>

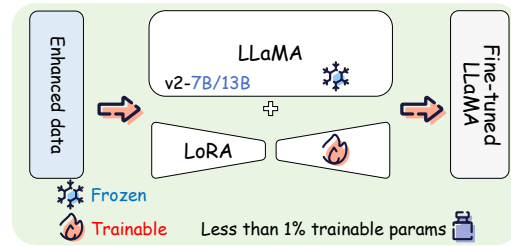


Figure 3: LLM Fine-tuning.

Therefore, this paper uses Low-Rank Adaptation (LoRA) (Hu et al., 2021) for fine-tuning. This technique only adds a low-rank (i.e., lower dimension) matrix  $\Delta W$  to the model's weight matrix  $W_0 \in \mathbb{R}^{d \times k}$ , while leaving most of the original model unchanged. LoRA provides an efficient way to fine-tune LLM when resources are limited or you want to retain pre-trained knowledge. The formula is as follows:

$$\begin{aligned} W_0 + \Delta W &= W_0 + BA, \\ B &\in \mathbb{R}^{d \times r}, A \in \mathbb{R}^{r \times k}, \end{aligned} \quad (5)$$

where,  $r \ll \min(d, k)$ . Finally, the parameters of the original LLaMA2 and the fine-tuning parameters obtained by LoRA are combined to obtain a fine-tuning model that can generate texts with certain discourse characteristics.

### 2.3.2 Stego generation

Stego generation is shown in Figure 1. Our stegos are generated based on Prompt and secret information bitstream control. The generation process is mainly composed of the probability generation module and the embedding module. The process  $PG$  and  $Em$  formulas of these modules are as follows:

$$\left\{ \begin{array}{l} PG : Ge(LM(I)) \rightarrow P \\ Em : match\ m_t\ \text{in}\ \{Rc(Trun(P))\} \end{array} \right\}, \quad (6)$$

$$i = Em(PG(I)), \quad (7)$$

where,  $I$  and  $P$  represent the index sequence of a given text and the probability distribution of the next token,  $P = [p^1, p^2, \dots, p^v]$ ,  $p^v$  represents the probability of the  $v$ -th token in the vocabulary, and  $|v|$  is the number of tokens in the vocabulary.  $LM(\cdot)$  and  $Ge(\cdot)$  represent the process of using fine-tuned LLM to generate vector representation and obtain token probability distribution.  $Rc(\cdot)$  and  $Trun(\cdot)$  represent the range coding and truncation process.  $match \circ in\{\cdot\}$  represents the process of matching the same prefix between the  $\circ$  and  $\{\cdot\}$ , and  $i$  is the index to generate the next token.

The probability generation module receives the content generated by the given Prompt or Prompt+part of generation. This module provides the embedding module with the probability distribution of the token to be generated. After receiving the probability distribution, the embedding module first samples and arranges the  $top\_k$  tokens to build the candidate pool  $CP$ . Then, range coding is performed for each token on the interval length of 0 to  $2^\alpha - 1$  according to the token probability in  $CP$ . Range coding is an information encoding method commonly used for lossless compression of data. It can be easily adapted to different probability distributions, making it very effective in many types of data compression tasks. In addition, since range coding is a lossless compression technology, the original data can be restored intact. Here we allocate different intervals according to the probability of the candidate pool token, and then take the  $\alpha$ -bit secret bit to determine a binary number and obtain the token corresponding to the matching interval. Then the beginning and the ending of the interval are matched to obtain a common prefix, which is the secret bit embedded at this moment. Therefore, the actual embedded secret information is the common prefix of the corresponding interval, not the  $\alpha$  bits. Loop the above process, the final stego will be obtained according to the inverse mapping. Algorithm 1 illustrates the secret embedding of LLMs.

**Probability generation module.** This module uses a fine-tuned LLM as an encoder for the autoregressive generation of text sequences. At the first moment, i.e.  $t = 1$ , the input is a

---

**Algorithm 1** Secret embedding of LLMs.

---

**Input:** Secret  $B = \{x, x, x, \dots, x\}, x \in \{0, 1\}$ ;  
Prompt.

**Output:** Discourse-controlled stego texts  $S = [t_{n+1}, t_{n+2}, \dots, \langle \text{EOS} \rangle]$  with secret.

- 1: Preparation for fine-tuning LLM;
  - 2: **while** Not the end of the secret bitstream **do**
  - 3:   Map typed Prompt to  $I_1 = [i_1, i_2, \dots, i_n]$ ;
  - 4:   **while** The generated token is not  $\langle \text{EOS} \rangle$  **do**
  - 5:     According to the probability generation module, encode  $I$  as  $E = [e_1, e_2, \dots, e_n]$ , and generate the probability distribution of the next token  $P$ ;
  - 6:     Sample all tokens and retain the  $top\_k$  tokens with higher probability, and constructing  $CP$ ;
  - 7:     Range coding is performed for each token on the interval length of 0 to  $2^\alpha - 1$  according to the token's probability in the  $CP$ ;
  - 8:     The  $\alpha$ -bit secret bitstream is taken to determine an integer and the corresponding token of the matching intervals is obtained;
  - 9:     According to the obtained token, use the dictionary  $D$  inverse mapping to find the corresponding index  $i$ ;
  - 10:     Add the index  $i$  to the existing index sequence, for example  $I_1 \leftarrow I_2 = [i_1, i_2, \dots, i_n, i_{n+1}]$ , and input it into the fine-tuned LLM to generate subsequent tokens;
  - 11:   **end while**
  - 12:   Matches the beginning and the ending of this interval to get the same prefix;
  - 13:   Delete the same prefix in the secret information at this moment, and embed it from the next digit of the same prefix in the secret information at the next moment;
  - 14: **end while**
  - 15: Get the final index sequence  $I_t = [i_1, i_2, \dots, i_n, i_{n+1}, i_{n+2}, \dots, i_{\langle \text{EOS} \rangle}]$ ;
  - 16: Inversely map  $[i_{n+1}, i_{n+2}, \dots, i_{\langle \text{EOS} \rangle}]$  generated in  $I_t$  to obtain the final  $S$ .
- 

given Prompt mapped to a dictionary index sequence  $I_1 = [i_1, i_2, \dots, i_n]$ , and then encoded into a vector representation  $E_1$ . At the second moment, i.e.  $t = 2$ , the index sequence  $I_2 =$

$[i_1, i_2, \dots, i_n, i_{n+1}]$  is the index  $i_{n+1}$  corresponding to Prompt and the final selection  $p_{n+1}^i$  at the first moment. Repeat until the index sequence  $I_t = [i_1, i_2, \dots, i_n, i_{n+1}, i_{n+2}, \dots, i_{<EOS>}]$  at time  $t$  is obtained. At this moment,  $[i_{n+1}, i_{n+2}, \dots, i_{<EOS>}]$  in  $I_t$  is the index sequence corresponding to the stego  $S$ .

**Embedding module.** After receiving the probability distribution  $P$  of the next token generated by the probability generation module, the embedding module first samples and truncates all tokens, and uses the retained tokens to construct the  $CP$ . Then mapping each token in the  $CP$  into intervals based on the probability and encode it. Then the corresponding interval is obtained based on the secret information, and the token corresponding to the target interval is obtained; and the same prefix of the beginning and the ending of the interval is matched, which is the secret information embedded at this moment. Using the decoder, the reverse mapping obtains the index  $i$  of the current token, which is input to the probability generation module at the next moment to continue generating probability distributions.

### 2.3.3 Bitstream extraction

After the authorized recipient Bob receives the stegos from the public channels, he extracts the secret information contained in them. Bitstream extraction and bitstream embedding are a pair of reciprocal operations. To ensure complete extraction of the bitstream, Alice and Bob need to use the same probability generation module, dictionary, and coding algorithm. The expression for the extraction process  $Ex$  is as follows:

$$\begin{cases} P = PG(I) \\ Ex : match \ i_{n+1} \text{ in } \{Rc(Trun(P))\} \end{cases}, \quad (8)$$

When the corresponding interval is obtained using the next token of the stego, the beginning and the ending of the range encoding will be matched, and the same prefix will be the current secret information. Algorithm 2 illustrates the secret bitstream extraction of LLsM.

## 3 Experiments

In this section, we show the comparison results of LLsM and existing schemes. The results show that LLsM has achieved superior performance in terms of text quality, statistical analysis, discourse

---

### Algorithm 2 Secret extraction of LLsM.

---

**Input:** Discourse-controlled stego texts  $S = [t_{n+1}, t_{n+2}, \dots, <EOS>]$  with secret.

**Output:** Secret  $B = \{x, x, x, \dots, x\}, x \in \{0, 1\}$ .

- 1: Prepare the probability generation module, dictionary  $D$ , and coding algorithm consistent with Algorithm 1;
  - 2: **while** Not the end of  $S$  **do**
  - 3:   Read the word  $t_{n+1}$  from  $S$  and map it to the index  $i_{n+1}$ ;
  - 4:   According to the probability generation module, input  $i_{n+1}$ , and generate the probability distribution  $P$  of the next token;
  - 5:   According to  $P$ , sample all tokens and retain  $top\_k$  tokens, and construct the  $CP$ ;
  - 6:   Use  $2^\alpha$  intervals to encode each token in the  $CP$ ;
  - 7:   **if**  $t_{n+i} \in S$  in  $CP$  **then**
  - 8:     According to the actual token, determine a certain interval. The same prefix of the beginning and the ending of the range coding at this moment is the secret bit stream at the current moment, and is added to  $B$ ;
  - 9:   **else**
  - 10:     The secret bitstream extraction process ends;
  - 11:   **end if**
  - 12: **end while**
  - 13: Get the final extracted secret bitstream  $B = \{x, x, x, \dots, x\}, x \in \{0, 1\}$ .
- 

matching, and anti-steganalysis. All experiments are run on NVIDIA GeForce RTX 4090 GPUs.

### 3.1 Settings

**Dataset.** We obtained a large amount of data from Wikipedia<sup>1</sup>, Twitter<sup>2</sup>, and GPT4 (OpenAI, 2023), and preprocessed and filtered the data. In addition, we used part of the publicly available data for training other LLM<sup>3</sup>, and finally obtained 108,771 texts, 392,478 tokens, and covered a dataset of nearly 100 different discourse characteristics for fine-tuning LLM.

**Model configuration.** We employed Meta LLaMA2 (Touvron et al., 2023) introduced in Section 2.3.1, and used the above dataset and LoRA to

<sup>1</sup><https://www.wikipedia.org/>

<sup>2</sup><https://twitter.com/>

<sup>3</sup><https://github.com/tloen/alpaca-lora/tree/main>

fine-tune LLaMA2, and the resulting fine-tuned LLM is used as the language model of LLsM. Specifically, LLsM adopted LLaMA2 7B (674 million parameters) and 13B (1.302 billion parameters) models. During the fine-tuning process, the rank of LoRA is 8, the normalized parameter is 16, the dropout is 0.05, the fine-tuned modules are  $Q$  and  $V$ , and the maximum sentence length is 512. The learning algorithm is AdamW (Loshchilov and Hutter, 2018), and the learning rate is initialized to  $1e-5$ . The batch size is set to 16, the micro-batch size is set to 8, and the training epoch is set to 3.

**Baselines.** We selected the prevalent works in recent years that demonstrated SOTA performance at different concealments as the baselines.

Robust perceptual concealment baselines: **(1) Tina-Fang** (Fang et al., 2017). It produces significantly better performance than modified linguistic steganography schemes. **(2) RNN-Stega** (Yang et al., 2019a). It has excellent generative performance in multiple datasets.

Robust statistical concealment baseline: **(3) ADG** (Zhang et al., 2021). Its superiority has been showed both mathematically and experimentally.

Related-task baseline (watermark): **(4) PLM-mark** (Li et al., 2023b). It utilizes pre-trained language models to provide the first secure and robust black-box watermarking scheme, protecting PLM’s intellectual property.

These schemes encompass the more comprehensive requirements of LS tasks and are conducive to comparing the generation effects of LLsM from different levels. The performance of these schemes has been widely recognized, so they were selected as representatives of the baseline for experiments.

**Evaluation metrics.** We comprehensively evaluate the performance of the solution in terms of text quality, statistical analysis, discourse matching, and anti-steganalysis.

In terms of text quality, we adopt **(1) PPL** (stego perplexity). PPL is often used to evaluate a language model’s ability to generate and understand texts (Wu et al., 2023). A lower PPL means that the model has better modeling capabilities for the distribution of this data (Ding et al., 2023). **(2)  $\Delta Pcs$**  (The difference between PPL of cover and stego (Yang et al., 2021)). A lower  $\Delta Pcs$  means that the model can better simulate the distribution of cover, which to a certain extent illustrates the strong concealment of stego.

In terms of statistical analysis, we adopt **(3) JSD** (Jensen-Shannon divergence). JSD is a method for measuring the difference between two probability distributions (Li et al., 2023a), which averages the KL divergence. A lower JSD means that the probability distributions of stego and cover are more similar. **(4)  $\Delta CS$**  (Cosine distance).  $\Delta CS$  is 1 minus the cosine similarity between stego and cover (Zhou et al., 2023), that is,  $\Delta CS = 1 - CS$ . **(5) ED** (Euclidean distance). When the text is represented as a dense vector, a smaller ED means that the stego is more similar to the cover. **(6) MD** (Manhattan distance). **(7)  $\Delta DP$**  (Dot product difference (Cai et al., 2021)).

In terms of discourse matching, we adopt **(8)  $\Delta LDA$**  (topic distribution difference (Bu et al., 2023)). **(9) MAUVE** (Pillutla et al., 2021). MAUVE is a metric for dialogue system evaluation that takes into account reply fluency, message consistency, and conversation quality. **(10) BLEU** (Bilingual evaluation understudy (Papineni et al., 2002)), which is a metric for machine translation that measures the similarity between the generated translation and the human reference translation. In LS, BLEU can measure the similarity between stego and cover. **(11) Rouge-L** (Lin, 2004). Rouge-L mainly evaluates the similarity between stego and cover by calculating the longest common subsequence. **(12) BERTScore** (Zhang et al., 2020). BERTScore considers the similarity between stego and cover at the word and segment level.

In terms of anti-steganalysis, we use the detection results of the high-performance deep-learning linguistic steganalysis methods **LS\_CNN** (Wen et al., 2019), **TS\_CSW** (Yang et al., 2020), **EILG** (Xu et al., 2023b) and **UP4LS** (Wang et al., 2023c): **(13) Acc** (Detection accuracy). **(14) F1**. The Acc and F1 formulas are shown in (Wang et al., 2023c).

### 3.2 Comparison with baselines

Faced with the need to generate texts with multiple discourse characteristics, the language model of the baselines has two training methods: One is to train "**Whole**" texts with multiple discourse characteristics to obtain a model that contains multiple discourse characteristics. The other is to train "**Individual**" texts with specific discourse characteristics to obtain multiple models containing specific discourse characteristics.

### 3.2.1 Text quality

Table 1 shows the comparison between LLMs and baselines in terms of the stego quality.

Table 1: Comparison between LLMs and baselines in terms of the quality of stego generation (perceptual concealment). **Red bold** represents the best performance. The parameters "bin" and "bit" in Tina-Fang and RNN-Stega are set to 1, 3, and 5 for experiments. "7B" and "13B" represent the parameter amount of the original LLaMA2 model,  $2^\alpha$  represents the number of intervals, and "Whole" and "Individual" represent as described in Section 3.2. "ER" represents the embedding rate in the current situation.

| Schemes                           |            |                          | PPL ↓         | $\Delta$ Pcs ↓ |
|-----------------------------------|------------|--------------------------|---------------|----------------|
| Tina-Fang<br>(Fang et al., 2017)  | Whole      | bin=1                    | 235.2707      | 227.5782       |
|                                   |            | bin=3                    | 269.3030      | 261.6106       |
|                                   |            | bin=5                    | 272.1803      | 264.4878       |
|                                   | Individual | bin=1                    | 61.1301       | 53.4376        |
|                                   |            | bin=3                    | 62.4138       | 54.7213        |
|                                   |            | bin=5                    | 65.2493       | 57.5568        |
| RNN-Stega<br>(Yang et al., 2019a) | Whole      | bit=1                    | 79.9866       | 72.2941        |
|                                   |            | bit=3                    | 99.3020       | 91.6096        |
|                                   |            | bit=5                    | 119.3254      | 111.6329       |
|                                   | Individual | bit=1                    | 14.2837       | 6.5912         |
|                                   |            | bit=3                    | 59.6795       | 51.9870        |
|                                   |            | bit=5                    | 83.0753       | 75.3828        |
| ADG<br>(Zhang et al., 2021)       | Whole      |                          | 197.4981      | 189.8056       |
|                                   | Individual |                          | 55.1914       | 47.4989        |
| PLMmark (Li et al., 2023b)        |            |                          | 18.7482       | 11.0557        |
| Ours                              | 7B         | $\alpha=2$ (ER: 0.4661)  | <b>4.7665</b> | 2.9337         |
|                                   |            | $\alpha=4$ (ER: 0.4085)  | 4.7865        | 2.9060         |
|                                   |            | $\alpha=8$ (ER: 1.0956)  | 7.6864        | <b>0.0061</b>  |
|                                   |            | $\alpha=16$ (ER: 1.1252) | 8.2682        | 0.5757         |
|                                   |            | $\alpha=32$ (ER: 1.1082) | 8.1843        | 0.4918         |
|                                   | 13B        | $\alpha=48$ (ER: 1.1254) | 8.2191        | 0.5267         |
|                                   |            | $\alpha=32$ (ER: 1.1064) | <b>8.4314</b> | 0.7389         |

According to the comparison results in Table 1, it can be found that text quality is as follows:

- The quality of the stegos generated by LLMs markedly surpasses that of the baselines. Particularly, when the original model is 7B and  $\alpha=8$ , the  $\Delta$ Pcs value is minimal. This shows that the stegos generated by LLMs can be more consistent with the linguistic characteristics of the cover training model, enhancing the perceptual concealment of the stegos.
- In the training way of the language model in the baselines, the PPL of the stegos generated by the "Whole" training is significantly higher than that of "Individual" training. This suggests that the "Whole" training hinders the language model's ability to capture diverse discourse characteristics in texts. While "Individual" training achieves lower PPL, it comes at the cost of requiring a multitude of models. Each model is limited to generating stegos with specific discourse characteristics, which severely limits practicality and scalability.

### 3.2.2 Statistical analysis

Table 2 shows the comparison between LLMs and baselines in terms of the statistical analysis between cover and stego.

According to the comparison results in Table 2, it can be found that in terms of statistical analysis:

- The stegos generated by LLMs can better simulate the statistical distribution of cover. Especially when the original model is 7B and  $\alpha=32/48$ , the statistical difference between cover and stego is the smallest, which shows that the stegos generated at this time best simulates the distribution of the cover, enhancing the statistical concealment of stegos.
- In the training way of the language model in the baselines, the metrics JSD,  $\Delta$ CS, ED, MD, and  $\Delta$ DP of the stegos generated by the "Whole" training are markedly higher than those of "Individual" training. This indicates that "Whole" training of the language model makes it difficult to learn the overall distribution of different texts, thereby the "Whole" training of the baselines is less controllable to a certain extent.

### 3.2.3 Discourse matching

Table 3 shows the comparison between LLMs and baselines in terms of the discourse matching of cover and stego.

According to the comparison results in Table 3, we observe that the stegos generated by LLMs has a better degree of discourse matching with cover. Specifically, when the original model is 13B,  $\alpha=32$ , the MAUVE metric indicates an improvement, surpassing 70%-80% of the baselines. Furthermore, when the original model is 7B,  $\alpha=32$ , the BLEU score shows a notable enhancement, exceeding 40%-50% of the baselines. Results show that the discourse controllability of LLMs in generating stegos is significantly superior to the baselines. It enhances the semantic concealment of stegos.

### 3.2.4 Anti-steganalysis ability

Table 4 shows the anti-steganalysis comparison of stegos generated by LLMs and baselines.

According to the comparison results in Table 4, it is found that compared with baselines, stegos generated by LLMs are more difficult to detect by high-performance steganalysis. Specifically, in the non-BERT-based LS\_CNN method, LLMs's stego detection accuracy is 30%-40% lower than that of

Table 2: Comparison between LLMs, LS-task baselines, and related-task baseline in terms of the statistical analysis between cover and stego (statistical concealment). The meanings expressed by "Whole", "Individual", "bin", "bit", and " $\alpha$ " are the same as those in Table 1. **Red bold** represents the best performance.

| Schemes                        |            |             | JSD ↓         | $\Delta$ CS ↓ | ED ↓          | MD ↓          | $\Delta$ DP ↓ |
|--------------------------------|------------|-------------|---------------|---------------|---------------|---------------|---------------|
| Tina-Fang (Fang et al., 2017)  | Whole      | bin=1       | 0.6343        | 0.9069        | 1.3468        | 17.9111       | 0.9069        |
|                                |            | bin=3       | 0.6334        | 0.9070        | 1.3468        | 17.8763       | 0.9070        |
|                                |            | bin=5       | 0.6338        | 0.9074        | 1.3471        | 17.7938       | 0.9074        |
|                                | Individual | bin=1       | 0.3964        | 0.2684        | 0.7327        | 12.5390       | 0.2684        |
|                                |            | bin=3       | 0.3953        | 0.3703        | 0.8606        | 11.3149       | 0.3703        |
|                                |            | bin=5       | 0.4022        | 0.3628        | 0.8519        | 13.2135       | 0.3628        |
| RNN-Stega (Yang et al., 2019a) | Whole      | bit=1       | 0.4151        | 0.0403        | 0.2839        | 7.5304        | 0.0403        |
|                                |            | bit=3       | 0.3938        | 0.0368        | 0.2713        | 7.3714        | 0.0368        |
|                                |            | bit=5       | 0.4077        | 0.0372        | 0.2729        | 7.4137        | 0.0372        |
|                                | Individual | bit=1       | 0.5484        | 0.1342        | 0.5180        | 11.1034       | 0.1342        |
|                                |            | bit=3       | 0.4150        | 0.0581        | 0.3408        | 7.8919        | 0.0581        |
|                                |            | bit=5       | 0.5159        | 0.0966        | 0.4395        | 10.4355       | 0.0966        |
| ADG (Zhang et al., 2021)       | Whole      | 0.4302      | 0.0318        | 0.2523        | 8.2321        | 0.0318        |               |
|                                | Individual | 0.5275      | 0.1468        | 0.5419        | 11.3048       | 0.1468        |               |
| PLMmark (Li et al., 2023b)     |            |             | 0.5376        | 0.1668        | 0.5776        | 9.9661        | 0.1668        |
| Ours                           | 7B         | $\alpha=2$  | 0.4766        | 0.0474        | 0.3080        | 8.6491        | 0.0474        |
|                                |            | $\alpha=4$  | 0.4721        | 0.0455        | 0.3018        | 8.5015        | 0.0455        |
|                                |            | $\alpha=8$  | 0.3886        | 0.0280        | 0.2367        | 6.4575        | 0.0280        |
|                                |            | $\alpha=16$ | 0.3849        | 0.0258        | 0.2273        | 6.3386        | 0.0258        |
|                                |            | $\alpha=32$ | 0.3848        | <b>0.0235</b> | <b>0.2168</b> | 6.2929        | <b>0.0235</b> |
|                                |            | $\alpha=48$ | <b>0.3846</b> | 0.0255        | 0.2260        | <b>6.2725</b> | 0.0255        |
|                                | 13B        | $\alpha=32$ | 0.4393        | 0.0368        | 0.2714        | 8.0344        | 0.0368        |

Table 3: Comparison between LLMs, LS-task baselines, and related-task baseline in terms of the discourse matching of cover and stego (semantic concealment). The meanings expressed by "Whole", "Individual", "bin", "bit", and " $\alpha$ " are the same as those in Table 1. **Red bold** represents the best performance. " $a \pm b$ " represents "average  $\pm$  standard deviation". For specific data, please see Appendix A for examples.

| Schemes                        |            |             | $\Delta$ LDA ↓    | MAUVE ↑ (%)                       | BLEU ↑ (%)                        | Rouge-L ↑ (%)                    | BERTScore ↑ (%)                  |
|--------------------------------|------------|-------------|-------------------|-----------------------------------|-----------------------------------|----------------------------------|----------------------------------|
| Tina-Fang (Fang et al., 2017)  | Whole      | bin=1       | 0.11964           | 2.15 $\pm$ 0.87                   | 0.90 $\pm$ 1.58                   | 0.45 $\pm$ 0.16                  | 42.58 $\pm$ 1.30                 |
|                                |            | bin=3       | 0.11964           | 1.96 $\pm$ 0.68                   | 0.90 $\pm$ 1.59                   | 0.53 $\pm$ 0.18                  | 41.65 $\pm$ 1.33                 |
|                                |            | bin=5       | 0.11964           | 2.23 $\pm$ 0.97                   | 0.90 $\pm$ 1.58                   | 0.51 $\pm$ 0.20                  | 43.02 $\pm$ 1.27                 |
|                                | Individual | bin=1       | 0.15950           | 0.59 $\pm$ 0.16                   | 21.79 $\pm$ 17.12                 | 4.07 $\pm$ 1.25                  | 47.59 $\pm$ 3.39                 |
|                                |            | bin=3       | 0.20424           | 0.60 $\pm$ 0.19                   | 22.03 $\pm$ 18.39                 | 3.88 $\pm$ 0.97                  | 47.21 $\pm$ 2.83                 |
|                                |            | bin=5       | 0.20424           | 0.51 $\pm$ 0.14                   | 22.18 $\pm$ 17.30                 | 3.46 $\pm$ 0.72                  | 47.77 $\pm$ 3.65                 |
| RNN-Stega (Yang et al., 2019a) | Whole      | bit=1       | 0.00062           | 12.73 $\pm$ 10.56                 | 1.87 $\pm$ 3.28                   | 7.95 $\pm$ 0.87                  | 52.57 $\pm$ 2.20                 |
|                                |            | bit=3       | 0.18919           | 11.97 $\pm$ 10.56                 | 1.83 $\pm$ 3.21                   | 7.55 $\pm$ 0.84                  | 52.36 $\pm$ 1.80                 |
|                                |            | bit=5       | 0.11969           | 15.22 $\pm$ 6.81                  | 1.76 $\pm$ 3.09                   | 6.85 $\pm$ 0.93                  | 51.58 $\pm$ 2.06                 |
|                                | Individual | bit=1       | 0.00009           | 0.53 $\pm$ 0.36                   | 24.54 $\pm$ 19.40                 | 9.73 $\pm$ 1.75                  | 36.64 $\pm$ 5.50                 |
|                                |            | bit=3       | 0.00012           | 0.54 $\pm$ 0.38                   | 25.78 $\pm$ 13.69                 | 10.78 $\pm$ 1.98                 | 37.44 $\pm$ 5.42                 |
|                                |            | bit=5       | 0.00008           | 0.55 $\pm$ 0.43                   | 32.36 $\pm$ 20.85                 | 10.71 $\pm$ 1.66                 | 36.54 $\pm$ 5.00                 |
| ADG (Zhang et al., 2021)       | Whole      | 0.15901     | 18.54 $\pm$ 13.89 | 2.72 $\pm$ 4.79                   | 8.66 $\pm$ 1.12                   | 47.55 $\pm$ 2.25                 |                                  |
|                                | Individual | 0.11962     | 0.79 $\pm$ 1.17   | 31.08 $\pm$ 22.53                 | 10.91 $\pm$ 3.11                  | 38.86 $\pm$ 4.06                 |                                  |
| PLMmark (Li et al., 2023b)     |            |             | 0.00009           | 7.22 $\pm$ 4.88                   | 0.15 $\pm$ 0.27                   | 3.23 $\pm$ 0.77                  | 43.50 $\pm$ 0.79                 |
| Ours                           | 7B         | $\alpha=2$  | 0.00010           | 30.13 $\pm$ 30.21                 | 70.78 $\pm$ 29.00                 | <b>12.97<math>\pm</math>3.38</b> | 60.67 $\pm$ 4.41                 |
|                                |            | $\alpha=4$  | <b>0.00004</b>    | 32.27 $\pm$ 22.00                 | 62.54 $\pm$ 34.43                 | 12.75 $\pm$ 3.23                 | 62.11 $\pm$ 4.15                 |
|                                |            | $\alpha=8$  | 0.00017           | 79.91 $\pm$ 26.75                 | 76.37 $\pm$ 31.85                 | 10.42 $\pm$ 2.82                 | <b>65.76<math>\pm</math>4.13</b> |
|                                |            | $\alpha=16$ | 0.00035           | 80.28 $\pm$ 26.43                 | 75.77 $\pm$ 32.22                 | 10.26 $\pm$ 2.30                 | 64.88 $\pm$ 4.13                 |
|                                |            | $\alpha=32$ | 0.00022           | 76.97 $\pm$ 26.47                 | <b>77.85<math>\pm</math>30.42</b> | 10.20 $\pm$ 2.41                 | 65.22 $\pm$ 4.61                 |
|                                |            | $\alpha=48$ | 0.00020           | 78.70 $\pm$ 25.51                 | 76.53 $\pm$ 31.71                 | 10.36 $\pm$ 2.47                 | 65.25 $\pm$ 4.78                 |
|                                | 13B        | $\alpha=32$ | 0.00039           | <b>88.38<math>\pm</math>24.12</b> | 1.55 $\pm$ 1.25                   | 10.08 $\pm$ 2.77                 | 61.66 $\pm$ 2.96                 |

Table 4: Steganalysis comparison of stegos generated by LLM, LS-task baselines, and related-task baseline. The meanings expressed by "Whole", "Individual", "bin", "bit", and " $\alpha$ " are the same as those in Table 1. **Red bold** represents the best performance. " $a\pm b$ " represents "average $\pm$ standard deviation". The unit is %.

| Schemes (%)                       |            |                  | LS_CNN                           |                                   | TS_CSW                           |                                  | EILG                             |                                  | UP4LS                            |                                  |
|-----------------------------------|------------|------------------|----------------------------------|-----------------------------------|----------------------------------|----------------------------------|----------------------------------|----------------------------------|----------------------------------|----------------------------------|
|                                   |            |                  | (Wen et al., 2019)               |                                   | (Yang et al., 2020)              |                                  | (Xu et al., 2023b)               |                                  | (Wang et al., 2023c)             |                                  |
|                                   |            |                  | Acc $\downarrow$                 | F1 $\downarrow$                   | Acc $\downarrow$                 | F1 $\downarrow$                  | Acc $\downarrow$                 | F1 $\downarrow$                  | Acc $\downarrow$                 | F1 $\downarrow$                  |
| Tina-Fang<br>(Fang et al., 2017)  | Whole      | bin=1            | 99.70 $\pm$ 0.29                 | 99.68 $\pm$ 0.31                  | 88.34 $\pm$ 21.22                | 91.01 $\pm$ 15.69                | 99.50 $\pm$ 0.25                 | 99.51 $\pm$ 0.25                 | 99.75 $\pm$ 0.06                 | 99.60 $\pm$ 0.09                 |
|                                   |            | bin=3            | 99.75 $\pm$ 0.16                 | 99.76 $\pm$ 0.15                  | 89.03 $\pm$ 20.58                | 92.39 $\pm$ 13.82                | 99.59 $\pm$ 0.17                 | 99.52 $\pm$ 0.66                 | 99.88 $\pm$ 0.10                 | 99.80 $\pm$ 0.15                 |
|                                   |            | bin=5            | 99.85 $\pm$ 0.20                 | 99.85 $\pm$ 0.19                  | 99.40 $\pm$ 0.40                 | 99.44 $\pm$ 0.38                 | 99.83 $\pm$ 0.17                 | 99.83 $\pm$ 0.25                 | 99.93 $\pm$ 0.10                 | 99.88 $\pm$ 0.15                 |
|                                   | Individual | bin=1            | 95.38 $\pm$ 0.81                 | 95.39 $\pm$ 0.75                  | 87.39 $\pm$ 17.52                | 90.80 $\pm$ 11.04                | 95.95 $\pm$ 0.66                 | 95.79 $\pm$ 0.54                 | 99.85 $\pm$ 0.19                 | 99.77 $\pm$ 0.29                 |
|                                   |            | bin=5            | 96.28 $\pm$ 0.44                 | 96.29 $\pm$ 0.43                  | 91.61 $\pm$ 5.06                 | 91.64 $\pm$ 4.64                 | 96.69 $\pm$ 0.41                 | 96.67 $\pm$ 0.82                 | 99.86 $\pm$ 0.12                 | 99.81 $\pm$ 0.17                 |
| RNN-Stega<br>(Yang et al., 2019a) | Whole      | bit=1            | 85.81 $\pm$ 1.93                 | 86.03 $\pm$ 1.40                  | 81.39 $\pm$ 1.70                 | 82.59 $\pm$ 1.62                 | 85.86 $\pm$ 0.50                 | 86.29 $\pm$ 0.89                 | 97.42 $\pm$ 0.44                 | 95.97 $\pm$ 0.67                 |
|                                   |            | bit=3            | 82.93 $\pm$ 2.18                 | 84.48 $\pm$ 2.20                  | 80.35 $\pm$ 2.38                 | 77.94 $\pm$ 3.04                 | 82.71 $\pm$ 0.17                 | 83.10 $\pm$ 1.02                 | 96.78 $\pm$ 0.82                 | 94.74 $\pm$ 1.34                 |
|                                   |            | bit=5            | 80.79 $\pm$ 1.01                 | 82.01 $\pm$ 1.15                  | 77.42 $\pm$ 2.10                 | 76.93 $\pm$ 3.07                 | 81.97 $\pm$ 0.41                 | 81.43 $\pm$ 1.57                 | 97.15 $\pm$ 0.37                 | 95.33 $\pm$ 0.75                 |
|                                   | Individual | bit=1            | 96.97 $\pm$ 1.28                 | 97.19 $\pm$ 1.16                  | 91.36 $\pm$ 1.87                 | 91.13 $\pm$ 2.41                 | 97.77 $\pm$ 0.25                 | 97.90 $\pm$ 0.24                 | 99.48 $\pm$ 0.39                 | 99.16 $\pm$ 0.59                 |
|                                   |            | bit=5            | 83.37 $\pm$ 2.49                 | 84.51 $\pm$ 2.76                  | 89.38 $\pm$ 3.84                 | 87.89 $\pm$ 5.10                 | 86.85 $\pm$ 0.25                 | 85.31 $\pm$ 1.45                 | 97.02 $\pm$ 1.40                 | 96.72 $\pm$ 1.22                 |
| ADG<br>(Zhang et al., 2021)       | Whole      | 82.38 $\pm$ 3.78 | 83.74 $\pm$ 2.82                 | 85.31 $\pm$ 16.51                 | 85.61 $\pm$ 15.98                | 87.88 $\pm$ 1.16                 | 87.95 $\pm$ 1.96                 | 98.99 $\pm$ 0.35                 | 98.46 $\pm$ 0.53                 |                                  |
|                                   | Individual | 85.86 $\pm$ 1.73 | 86.35 $\pm$ 1.82                 | 82.23 $\pm$ 2.40                  | 82.08 $\pm$ 2.96                 | 84.86 $\pm$ 1.74                 | 84.10 $\pm$ 1.80                 | 98.34 $\pm$ 0.39                 | 97.41 $\pm$ 0.58                 |                                  |
| PLMmark (Li et al., 2023b)        |            |                  | 97.07 $\pm$ 1.79                 | 97.03 $\pm$ 1.78                  | 97.35 $\pm$ 0.87                 | 97.37 $\pm$ 0.87                 | 98.01 $\pm$ 0.74                 | 98.07 $\pm$ 0.73                 | 99.76 $\pm$ 0.22                 | 99.54 $\pm$ 0.46                 |
| Ours                              | 7B         | $\alpha=2$       | 98.64 $\pm$ 0.92                 | 98.60 $\pm$ 0.95                  | 98.81 $\pm$ 1.83                 | 98.75 $\pm$ 1.93                 | 99.92 $\pm$ 0.17                 | 99.92 $\pm$ 0.11                 | 99.85 $\pm$ 0.30                 | 99.85 $\pm$ 0.30                 |
|                                   |            | $\alpha=4$       | 77.66 $\pm$ 5.36                 | 79.89 $\pm$ 3.18                  | 72.01 $\pm$ 5.97                 | 73.78 $\pm$ 9.36                 | 81.14 $\pm$ 0.50                 | 81.25 $\pm$ 1.18                 | 88.04 $\pm$ 0.29                 | 79.03 $\pm$ 1.08                 |
|                                   |            | $\alpha=8$       | 75.19 $\pm$ 1.55                 | 75.89 $\pm$ 2.41                  | 69.23 $\pm$ 4.94                 | 73.93 $\pm$ 3.75                 | 79.98 $\pm$ 0.33                 | 79.99 $\pm$ 1.07                 | 83.73 $\pm$ 0.43                 | 74.23 $\pm$ 1.52                 |
|                                   |            | $\alpha=16$      | 59.50 $\pm$ 2.77                 | 60.15 $\pm$ 10.59                 | 56.82 $\pm$ 4.09                 | 64.21 $\pm$ 10.03                | 67.25 $\pm$ 3.23                 | 68.04 $\pm$ 1.53                 | 75.40 $\pm$ 0.37                 | 50.84 $\pm$ 5.16                 |
|                                   | 13B        | $\alpha=32$      | 59.21 $\pm$ 5.47                 | 60.54 $\pm$ 11.10                 | 55.04 $\pm$ 3.97                 | 60.77 $\pm$ 11.62                | 63.69 $\pm$ 2.07                 | <b>61.47<math>\pm</math>2.27</b> | 74.01 $\pm$ 1.52                 | 43.97 $\pm$ 9.51                 |
|                                   |            | $\alpha=48$      | 59.35 $\pm$ 1.25                 | 59.99 $\pm$ 5.51                  | <b>54.05<math>\pm</math>4.72</b> | 61.68 $\pm$ 11.17                | <b>62.28<math>\pm</math>0.50</b> | 62.66 $\pm$ 2.31                 | 71.97 $\pm$ 0.64                 | 50.02 $\pm$ 3.45                 |
|                                   |            | $\alpha=32$      | <b>58.00<math>\pm</math>2.37</b> | <b>56.08<math>\pm</math>13.79</b> | 54.98 $\pm$ 3.14                 | 59.17 $\pm$ 11.37                | 65.51 $\pm$ 2.23                 | 66.78 $\pm$ 3.91                 | <b>71.40<math>\pm</math>0.65</b> | 40.24 $\pm$ 7.67                 |
|                                   |            | $\alpha=32$      | 59.74 $\pm$ 2.93                 | 56.95 $\pm$ 9.98                  | 55.73 $\pm$ 3.38                 | <b>58.70<math>\pm</math>9.14</b> | 64.35 $\pm$ 0.91                 | 63.74 $\pm$ 1.89                 | 88.61 $\pm$ 3.51                 | <b>14.02<math>\pm</math>6.48</b> |

baselines. Furthermore, within the BERT-based UP4LS method, LLM's stego detection accuracy is 20%-30% lower than that of baselines. This shows that LLM greatly increases the detection difficulty of steganalysis and is more conducive to the success of covert communication.

### 3.3 Long stegos by LLM

In addition, we also perform LLM in generating longer stegos. Examples are shown in Table 5.

According to the results in Table 5, the long stegos generated by LLM are relatively smooth, and the discourse characteristics are more in line with the guidance of Prompt. Since long stego generation is not the focus of this study, we will not go into details here.

## 4 Related Work

The construction of language models and their encoding ways are pivotal in determining the concealment and quality of stegos. Focusing on these two key aspects, researchers have developed various steganography schemes (Ding et al., 2023) (Yang et al., 2021) (Wang et al., 2023b) (Xiang et al., 2023) (Yang et al., 2023). Fang et al. (Fang et al., 2017) proposed an LSTM-based steganography scheme. This scheme segments the vocabulary into several sets based on bit blocks. It then selects tokens with the highest probability that corresponds to the secret information from the candidate pool, thereby enhancing the embedding capacity and ensuring perceptual concealment. Ding et al.

(Ding et al., 2023) combined the conditional generation strategy with the replacement technique, using text sequences as auxiliary data in the stego generation process to enhance the embedding capabilities. Yang et al. (Yang et al., 2019a) and (Yang et al., 2021) designed RNN-Stega and VAE-Stega steganography schemes. These schemes respectively use extensive cover to train their language models, and then encode each word based on the conditional probability distribution, employing fixed-length and variable-length encoding in RNN-Stega, and Huffman and arithmetic coding in VAE-Stega. Experimental results show that both schemes achieve excellent performance in terms of perceptual concealment and statistical concealment. To further reduce the distribution difference between cover and stego, Zhang et al. (Zhang et al., 2021) constructed a provably secure ADG scheme. It recursively embeds information via adaptive dynamic grouping. This scheme's robust statistical concealment has been verified theoretically and experimentally. Zhou et al. (Zhou et al., 2021) used a Generative Adversarial Network to design an adaptive probability distribution steganography scheme.

To improve semantic concealment, Li et al. (Li et al., 2021) put forward a steganography scheme based on the knowledge graph. This scheme encodes entities and relationships, and the multiple sentences generated show overall coherence and relevance while ensuring quality. Yang et al. (Yang et al., 2023) utilized semantic information encod-

Table 5: Examples of long stegos generated by LLMs.

| Secret & Bitstream  | Prompt   | Stegos  | PPL↓   | ΔLDA↓   |
|---|--|---|--------|---------|
| <b>Secret:</b><br><u>Multimedia</u><br><br><b>Bitstream:</b><br>010011010111010101<br>101100011101000110<br>100101101101011001<br>010110010001101001<br>01100001 (80bit)  | Introduction to Shakespeare's writing style.                       | Shakespeare's writing style is unique and unmatched by any other writer in history. His plays are notable for their richness and variety, their use of vivid imagery and metaphor, their powerful characters and their insight into the human condition. Shakespeare's use of iambic pentameter, for example, adds to the rhythm and beauty of his verse, while his use of puns and wordplay adds to the humor and wit of his plays. His characters are complex and multifaceted, and his use of language to explore their emotions and motivations is unparalleled. Shakespeare's writing style is also notable for its use of language to explore themes of love, loss, betrayal, and redemption. His plays are filled with powerful imagery and metaphors that help to bring these themes to life. Shakespeare's writing style is also notable for its use of language to explore the human condition. His characters are complex and multifaceted, and his use of language to explore their emotions and motivations is unparalleled. | 2.3081 | 0.00003 |
| <b>Secret:</b><br><u>Love and peace</u><br><br><b>Bitstream:</b><br>010011000110111101<br>110110011001010010<br>000001100'00101101<br>110011001000010000<br>00111000001100101'<br>011000010110001101<br>100101 (114bit) | Discuss the causes of the Great Depression.                        | The Great Depression was a severe economic downturn that lasted from 1929 to 1939. It was the worst economic depression in the history of the United States and it affected many countries around the world. The causes of the Great Depression are numerous and complex, but some of the main factors include overproduction, the bursting of the stock market bubble, banking failures, and government policies. One of the primary causes of the Great Depression was overproduction. The United States economy was booming in the 1920s, and many businesses and industries expanded their production to meet the growing demand. However, this resulted in an oversupply of goods and services, which led to a decrease in prices and a decrease in demand. This decrease in demand caused a drop in profits, which led to businesses cutting back on production and laying off workers.   | 2.1451 | 0.00004 |
|   | Explain the use of word embeddings in Natural Language Processing. | Word embeddings are a form of representation learning in natural language processing (NLP). Word embeddings are vectors of real numbers that represent the meaning of words. These vectors are learned from large amounts of text data and can be used to model the relationship between words and their contexts. Word embeddings can be used in various NLP tasks such as sentiment analysis, machine translation, and text classification.   | 3.3995 | 0.00006 |
|   | Give some strategies for getting over a fear of public speaking.   | Public speaking is a common fear for many people, and it can be difficult to overcome. Here are some strategies that can help: 1. Practice: The more you practice public speaking, the more comfortable you will become. Start by practicing in front of a small group of friends or family members, and gradually work your way up to larger audiences. 2. Visualize: Before giving a speech, visualize yourself giving a successful presentation. Imagine yourself confidently delivering your speech, and see yourself receiving positive feedback from the audience. 3. Breathe: Take deep, slow breaths before giving a speech.  | 2.0459 | 0.00007 |

ing to embed secret information, realizing the effect of maintaining semantics and increasing the embedding capacity during the translation process. Wang et al. (Wang et al., 2023b) leveraged the relevance of social network context to enhance contextual semantic relevance while maintaining existing schemes' embedding rates. Xiang et al. (Xiang et al., 2023) generated semantically consistent stegos by constructing a grammar-controlled paraphrase generation model and a grammar bin encoding strategy. This scheme maintained a high level of semantic coherence.

## 5 Conclusion

To improve the controllability of stego generation and improve their concealment, this paper proposes the LLM-based generative linguistic steganography scheme. This scheme constructed a dataset with rich discourse characteristics to fine-tune an open-source LLM. Then, We employ range coding on the sampled candidate pool to simulate the distribution of cover. Furthermore, this scheme inputs the information expected to obtain specific discourse characteristics into the fine-tuned LLM together with secret information, ensuring the degree of discourse matching of the generated stego. Experi-

ments show that the scheme proposed in this paper has achieved excellent performance in terms of text quality, statistical analysis, discourse matching, and anti-steganalysis. Notably, we also give an example of LLMs generating longer stego, demonstrating its potential advantages in long LS tasks. Last but not least, since the research focus of this paper is to improve the controllability and concealment of stego generation, there is not much elaboration and optimization in terms of fine-tuning the dataset and embedding rate.

In the next work, we will concentrate on fine-tuning the dataset and instruction optimization in LLM-based LS to further improve the concealment, text quality, discourse matching, and controllability of the stego. Given the limited related studies on long LS and stego diversity, we will also conduct in-depth research on high-quality search algorithms to improve the length and diversity of stego while ensuring text quality. We also recognize a gap in the steganalysis of stegos generated by LLMs. Current linguistic steganalysis tools struggle to accurately identify such texts. Addressing this, our future research will include developing LLM-based linguistic steganalysis techniques to improve the detection capabilities against stegos.

## Acknowledgements

This research was funded by the National Natural Science Foundation of China under Grant U21B2020 and in part by BUPT Excellent Ph.D. Students Foundation under Grant CX2023120.

## References

- Yuyan Bu, Qiang Sheng, Juan Cao, Peng Qi, Danding Wang, and Jintao Li. 2023. Combating online misinformation videos: Characterization, detection, and future directions. In *Proceedings of the 31st ACM International Conference on Multimedia (ACM MM)*, pages 8770–8780.
- Xingyu Cai, Jiayi Huang, Yuchen Bian, and Kenneth Church. 2021. Isotropy in the contextual embedding space: Clusters and manifolds. In *Proceedings of International Conference on Machine Learning (ICML)*.
- Changhao Ding, Zhangjie Fu, Qi Yu, Fan Wang, and Xianyi Chen. 2023. Joint linguistic steganography with bert masked language model and graph attention network. *IEEE Transactions on Cognitive and Developmental Systems*, page 1.
- Tina Fang, Martin Jaggi, and Katerina Argyraki. 2017. Generating steganographic text with lstms. In *Proceedings of the 55th Annual Meeting of the Association for Computational Linguistics- Student Research Workshop*, pages 100–106.
- Edward J. Hu, Yelong Shen, Phillip Wallis, Zeyuan Allen-Zhu, Yuanzhi Li, Shean Wang, Lu Wang, and Weizhu Chen. 2021. Lora: Low-rank adaptation of large language models. In *arXiv preprint*.
- Lin Huo and Yuchuan Xiao. 2016. Synonym substitution-based steganographic algorithm with vector distance of two-gram dependency collocations. In *Proceeding of the IEEE International Conference on Computer and Communications*, pages 2776–2780.
- MiYoung Kim, Osmar Zaiane, and Randy Goebel. 2010. Natural language watermarking based on syntactic displacement and morphological division. In *Proceeding of the 34th Annual IEEE Computer Software and Applications Conference Workshops*, pages 164–169.
- Jingzhi Li, Fengling Li, Lei Zhu, Hui Cui, and Jingjing Li. 2023a. Prototype-guided knowledge transfer for federated unsupervised cross-modal hashing. In *Proceedings of the 31st ACM International Conference on Multimedia (ACM MM)*, pages 1013–1022.
- Peixuan Li, Pengzhou Cheng, Fangqi Li, Wei Du, Haodong Zhao, and Gongshen Liu. 2023b. Plm-mark: a secure and robust black-box watermarking framework for pre-trained language models. In *Proceedings of the Thirty-Seventh AAAI Conference on Artificial Intelligence*, pages 14991–14999.
- Yamin Li, Jun Zhang, Zhongliang Yang, and Ru Zhang. 2021. Topic-aware neural linguistic steganography based on knowledge graphs. *ACM/IMS Transactions on Data Science*, 2(2):1–13.
- Chin-Yew Lin. 2004. Rouge: A package for automatic evaluation of summaries. *Text summarization branches out*, pages 74–81.
- Ilya Loshchilov and Frank Hutter. 2018. Decoupled weight decay regularization. In *Proceeding of International Conference on Learning Representations (ICLR)*.
- Tianhe Lu, Gongshen Liu, Ru Zhang, and Tianjie Ju. 2023. Neural linguistic steganography with controllable security. In *Proceeding of 2023 International Joint Conference on Neural Networks (IJCNN)*, pages 1–8.
- Zicong Luo, Sheng Li, Guobiao Li, Zhenxing Qian, and Xinpeng Zhang. 2023. Securing fixed neural network steganography. In *Proceedings of the 31st ACM International Conference on Multimedia (ACM MM)*, pages 7943–7951.
- Arya D. McCarthy and Giovanna Maria Dora Dore. 2023. Theory-grounded computational text analysis. In *Proceedings of the 61st Annual Meeting of the Association for Computational Linguistics (Volume 2: Short Papers)*, pages 1586–1594.
- OpenAI. 2023. Gpt-4 technical report. *arXiv preprint*.
- Kishore Papineni, Salim Roukos, Todd Ward, and Wei-Jing Zhu. 2002. Bleu: a method for automatic evaluation of machine translation. In *Proceedings of the 40th annual meeting of the Association for Computational Linguistics (ACL)*, pages 311–318.
- Yinyin Peng, Donghui Hu, Yaofei Wang, Kejiang Chen, Gang Pei, and Weiming Zhang. 2023. Stegaddpm: Generative image steganography based on denoising diffusion probabilistic model. In *Proceedings of the 31st ACM International Conference on Multimedia (ACM MM)*, pages 7143–7151.
- Krishna Pillutla, Swabha Swayamdipta, Rowan Zellers, John Thickstun, Sean Welleck, Yejin Choi, and Zaid Harchaoui. 2021. Mauve: Measuring the gap between neural text and human text using divergence frontiers. In *Proceedings of the 35th Conference on Neural Information Processing Systems (NIPS)*, volume 34, pages 4816–4828.
- C E. Shannon. 1949. Communication theory of secrecy systems. *The Bell system technical journal*, 28(4):656–715.
- Hugo Touvron, Louis Martin, Kevin Stone, Peter Albert, Anjad Almahairi, Yasmine Babaei, Soumya Batra, Nikolay Bashlykov, Shruti Bhosale, Prajjwal Bhargava, Dan Bikel, Lukas Blecher, Cristian Canton Ferrer, Moya Chen, Guillem Cucurull, David Esioiu, Jude Fernandes, Jeremy Fu, Wenyin Fu, Brian Fuller, Cynthia Gao, Vedanuj Goswami, Naman

- Goyal, Anthony Hartshorn, Saghar Hosseini, Rui Hou, Hakan Inan, Marcin Kardas, Viktor Kerkez, Madian Khabsa, Isabel Kloumann, Artem Korenev, Punit Singh Koura, Marie-Anne Lachaux, Thibaut Lavril, Diana Liskovich Jenya Lee, Yinghai Lu, Yun-ting Mao, Xavier Martinet, Todor Mihaylov, Pushkar Mishra, Igor Molybog, Yixin Nie, Andrew Poulton, Jeremy Reizenstein, Rashi Rungta, Kalyan Saladi, Alan Schelten, Ruan Silva, Eric Michael Smith, Rannan Subramanian, Xiaoqing Ellen Tan, Binh Tang, Ross Taylor, Adina Williams, Jian Xiang Kuan, Puxin Xu, Zheng Yan, Iliyan Zarov, Yuchen Zhang, Angela Fan, Melanie Kambadur, Sharan Narang, Arelieu Rodriguez, Robert Stojnic, Sergey Edunov, and Thomas Scialom. 2023. *Llama 2: Open foundation and fine-tuned chat models*. *arXiv preprint*.
- Huili Wang, Zhongliang Yang, Jinshuai Yang, Cheng Chen, and Yongfeng Huang. 2023a. Linguistic steganalysis in few-shot scenario. *IEEE Transactions on Information Forensics and Security*, 18:4870–4882.
- Huili Wang, Zhongliang Yang, Jinshuai Yang, Yue Gao, and Yongfeng Huang. 2023b. Hi-stega: A hierarchical linguistic steganography framework combining retrieval and generation. In *Proceeding of International Conference on Neural Information Processing (ICONIP)*, pages 41–54.
- Yihao Wang, Ruiqi Song, Ru Zhang, and Jianyi Liu. 2023c. *Up4ls: User profile constructed by multiple attributes for enhancing linguistic steganalysis*. *arXiv preprint*.
- Yihao Wang, Ru Zhang, and Jianyi Liu. 2023d. RLSDTs: Reinforcement-learning linguistic steganalysis in distribution-transformed scenario. *IEEE Signal Processing Letters*, 30:1232–1236.
- Juan Wen, Xuejing Zhou, Ping Zhong, and Yiming Xue. 2019. Convolutional neural network based text steganalysis. *IEEE Signal Processing Letters*, 26(3):460–464.
- Xiaoxia Wu, Cheng Li, Reza Yazdani Aminabadi, Zhewei Yao, and Yuxiong He. 2023. Understanding int4 quantization for language models: latency speedup, composability, and failure cases. In *Proceedings of International Conference on Machine Learning (ICML)*, pages 37524–37539.
- Lingyun Xiang, Chengfu Ou, and Daojian Zeng. 2023. Linguistic steganography: Hiding information in syntax space. *IEEE Signal Processing Letters*, 31:261–265.
- Danni Xu, Shaojing Fan, and Mohan Kankanhalli. 2023a. Combating misinformation in the era of generative ai models. In *Proceedings of the 31st ACM International Conference on Multimedia (ACM MM)*, pages 9291–9298.
- Qiong Xu, Ru Zhang, and Jianyi Liu. 2023b. Linguistic steganalysis by enhancing and integrating local and global features. *IEEE Signal Processing Letters*, 30:16–20.
- Jinshuai Yang, Zhongliang Yang, Jiajun Zou, Haoqin Tu, and Yongfeng Huang. 2022. Linguistic steganalysis towards social network. *IEEE Transactions on Information Forensics and Security*, 18:859–871.
- Tianyu Yang, Hanzhou Wu, Biao Yi, Guorui Feng, and Xinpeng Zhang. 2023. Semantic-preserving linguistic steganography by pivot translation and semantic-aware bins coding. *IEEE Transactions on Dependable and Secure Computing*, 21(1):139–152.
- Zhongliang Yang, Xiaoqing Guo, Ziming Chen, Yongfeng Huang, and Yujin Zhang. 2019a. Rnnstega: Linguistic steganography based on recurrent neural networks. *IEEE Transactions on Information Forensics and Security*, 14(5):1280–1295.
- Zhongliang Yang, Yongfeng Huang, and Yujin Zhang. 2020. Ts-csw: text steganalysis and hidden capacity estimation based on convolutional sliding windows. *Multimedia Tools and Applications*, 79:18293–18316.
- Zhongliang Yang, Ke Wang, Jian Li, Yongfeng Huang, and Yujin Zhang. 2019b. Ts-rnn: Text steganalysis based on recurrent neural networks. *IEEE Signal Processing Letters*, 26(12):1743–1747.
- Zhongliang Yang, Siyu Zhang, Yuting Hu, Zhiwen Hu, and Yongfeng Huang. 2021. Vae-stega: linguistic steganography based on variational auto-encoder. *IEEE Transactions on Information Forensics and Security*, 16:880–895.
- Siyu Zhang, Zhongliang Yang, Jinshuai Yang, and Yongfeng Huang. 2021. Provably secure generative linguistic steganography. In *Proceeding of the International Joint Conference on Natural Language Processing (ACL-IJCNLP)*, pages 3046–3055.
- Tianyi Zhang, Varsha Kishore, Felix Wu, Kilian Q. Weinberger, and Yoav Artzi. 2020. Bertscore: Evaluating text generation with bert. In *Proceedings of the 35th Conference on Neural Information Processing Systems (NIPS)*.
- Xuejing Zhou, Wanli Peng, Boya Yang, Juan Wen, Yiming Xue, and Ping Zhong. 2021. Linguistic steganography based on adaptive probability distribution. *IEEE Transactions on Dependable and Secure Computing*, 19(5):2982–2997.
- Ziqi Zhou, Shengshan Hu, Minghui Li, Hangtao Zhang, Yechao Zhang, and Hai Jin. 2023. Advclip: Downstream-agnostic adversarial examples in multimodal contrastive learning. In *Proceedings of the 31st ACM International Conference on Multimedia (ACM MM)*, pages 6311–6320.

## A Appendix A

Table 6: Comparison of MAUVE evaluation LLMs, LS-task baselines, and related-task baseline. The meanings expressed by "Whole", "Individual", "bin", "bit", and " $\alpha$ " are the same as those in Table 1. **Red bold** represents the best performance. " $a\pm b$ " represents "average $\pm$ standard deviation". The unit is %. Due to space limitations, this table only presents the generation performances on 10 discourse characteristic datasets.

| MAUVE $\uparrow$ (%)              |            |             | Admin | Andersen | Dickens | Education | Engineer | Geography | History | Literature | Movie | Music             | All (avg $\pm$ std)               |
|-----------------------------------|------------|-------------|-------|----------|---------|-----------|----------|-----------|---------|------------|-------|-------------------|-----------------------------------|
| Tina-Fang<br>(Fang et al., 2017)  | Whole      | bin=1       | 2.35  | 0.77     | 0.62    | 2.36      | 2.35     | 2.35      | 3.67    | 2.35       | 2.35  | 2.35              | 2.15 $\pm$ 0.87                   |
|                                   |            | bin=3       | 2.14  | 0.75     | 0.77    | 2.17      | 2.14     | 2.14      | 3.00    | 2.15       | 2.15  | 2.15              | 1.96 $\pm$ 0.68                   |
|                                   |            | bin=5       | 2.39  | 0.81     | 0.58    | 2.42      | 2.39     | 2.39      | 4.10    | 2.42       | 2.39  | 2.42              | 2.23 $\pm$ 0.97                   |
|                                   | Individual | bin=1       | 0.41  | 0.59     | 0.62    | 0.65      | 0.41     | 0.93      | 0.41    | 0.59       | 0.65  | 0.65              | 0.59 $\pm$ 0.16                   |
|                                   |            | bin=3       | 0.63  | 0.54     | 0.53    | 0.41      | 0.41     | 0.62      | 0.65    | 1.03       | 0.41  | 0.78              | 0.60 $\pm$ 0.19                   |
|                                   |            | bin=5       | 0.41  | 0.52     | 0.59    | 0.41      | 0.41     | 0.41      | 0.41    | 0.83       | 0.65  | 0.41              | 0.51 $\pm$ 0.14                   |
| RNN-Stega<br>(Yang et al., 2019a) | Whole      | bit=1       | 3.69  | 27.68    | 14.82   | 14.11     | 4.22     | 4.23      | 4.39    | 32.60      | 4.68  | 16.92             | 12.73 $\pm$ 10.56                 |
|                                   |            | bit=3       | 3.68  | 24.68    | 12.72   | 15.93     | 3.88     | 3.79      | 3.92    | 31.99      | 4.18  | 14.88             | 11.97 $\pm$ 10.56                 |
|                                   |            | bit=5       | 11.13 | 18.95    | 13.19   | 13.94     | 11.17    | 11.16     | 11.24   | 33.04      | 11.62 | 16.73             | 15.22 $\pm$ 6.81                  |
|                                   | Individual | bit=1       | 0.41  | 1.54     | 0.45    | 0.41      | 0.41     | 0.41      | 0.41    | 0.41       | 0.41  | 0.41              | 0.53 $\pm$ 0.36                   |
|                                   |            | bit=3       | 0.41  | 1.63     | 0.46    | 0.41      | 0.41     | 0.41      | 0.41    | 0.41       | 0.41  | 0.41              | 0.54 $\pm$ 0.38                   |
|                                   |            | bit=5       | 0.41  | 1.78     | 0.48    | 0.41      | 0.41     | 0.41      | 0.41    | 0.41       | 0.41  | 0.41              | 0.55 $\pm$ 0.43                   |
| ADG<br>(Zhang et al., 2021)       | Whole      | 28.26       | 13.74 | 7.89     | 35.86   | 7.91      | 7.90     | 7.98      | 45.83   | 7.97       | 22.03 | 18.54 $\pm$ 13.89 |                                   |
|                                   | Individual | 4.13        | 0.46  | 0.41     | 0.41    | 0.41      | 0.41     | 0.41      | 0.41    | 0.41       | 0.41  | 0.79 $\pm$ 1.17   |                                   |
| PLMmark (Li et al., 2023b)        |            |             | 0.69  | 0.49     | 5.51    | 12.87     | 5.51     | 5.51      | 5.51    | 13.43      | 9.04  | 13.63             | 7.22 $\pm$ 4.88                   |
| Ours                              | 7B         | $\alpha=2$  | 4.79  | 1.39     | 32.33   | 5.77      | 82.10    | 13.78     | 19.87   | 85.42      | 26.13 | 29.71             | 30.13 $\pm$ 30.21                 |
|                                   |            | $\alpha=4$  | 6.92  | 1.03     | 47.87   | 22.14     | 54.36    | 47.62     | 21.11   | 68.41      | 17.34 | 35.91             | 32.27 $\pm$ 22.00                 |
|                                   |            | $\alpha=8$  | 42.64 | 20.39    | 87.17   | 80.57     | 99.83    | 99.03     | 94.56   | 87.81      | 98.22 | 88.91             | 79.91 $\pm$ 26.75                 |
|                                   |            | $\alpha=16$ | 41.81 | 23.14    | 99.32   | 90.06     | 83.37    | 98.26     | 86.02   | 98.46      | 99.77 | 82.63             | 80.28 $\pm$ 26.43                 |
|                                   |            | $\alpha=32$ | 41.57 | 21.25    | 89.99   | 93.56     | 91.44    | 97.27     | 63.91   | 94.97      | 96.53 | 79.22             | 76.97 $\pm$ 26.47                 |
|                                   | 13B        | $\alpha=48$ | 42.35 | 22.61    | 96.52   | 83.79     | 99.83    | 88.40     | 91.21   | 79.46      | 94.84 | 87.98             | 78.70 $\pm$ 25.51                 |
|                                   |            | $\alpha=32$ | 64.38 | 27.18    | 99.24   | 100.00    | 98.77    | 96.75     | 99.31   | 99.93      | 98.28 | 99.98             | <b>88.38<math>\pm</math>24.12</b> |

Table 7: Comparison of BERTScore evaluation LLMs, LS-task baselines, and related-task baseline. The meanings expressed by "Whole", "Individual", "bin", "bit", and " $\alpha$ " are the same as those in Table 1. **Red bold** represents the best performance. " $a\pm b$ " represents "average $\pm$ standard deviation". The unit is %. Due to space limitations, this table only presents the generation performances on 10 discourse characteristic datasets.

| BERTScore $\uparrow$ (%)          |            |             | Admin | Andersen | Dickens | Education | Engineer | Geography | History | Literature | Movie | Music            | All (avg $\pm$ std)              |
|-----------------------------------|------------|-------------|-------|----------|---------|-----------|----------|-----------|---------|------------|-------|------------------|----------------------------------|
| Tina-Fang<br>(Fang et al., 2017)  | Whole      | bin=1       | 41.22 | 41.87    | 43.65   | 41.68     | 44.31    | 41.82     | 41.49   | 44.08      | 41.48 | 44.20            | 42.58 $\pm$ 1.30                 |
|                                   |            | bin=3       | 40.53 | 41.11    | 42.74   | 40.31     | 43.10    | 40.68     | 40.75   | 43.04      | 40.50 | 43.74            | 41.65 $\pm$ 1.33                 |
|                                   |            | bin=5       | 42.46 | 42.43    | 44.30   | 42.05     | 44.67    | 42.41     | 41.56   | 44.06      | 41.58 | 44.72            | 43.02 $\pm$ 1.27                 |
|                                   | Individual | bin=1       | 41.10 | 47.30    | 43.25   | 50.33     | 52.90    | 48.53     | 48.98   | 48.43      | 46.25 | 48.85            | 47.59 $\pm$ 3.39                 |
|                                   |            | bin=3       | 41.92 | 50.68    | 43.79   | 49.96     | 48.99    | 49.48     | 47.55   | 47.69      | 45.16 | 46.86            | 47.21 $\pm$ 2.83                 |
|                                   |            | bin=5       | 40.90 | 48.64    | 43.71   | 48.56     | 53.35    | 48.27     | 45.07   | 48.11      | 49.79 | 51.26            | 47.77 $\pm$ 3.65                 |
| RNN-Stega<br>(Yang et al., 2019a) | Whole      | bit=1       | 54.73 | 50.47    | 53.90   | 55.77     | 53.87    | 49.57     | 49.63   | 53.91      | 51.33 | 52.56            | 52.57 $\pm$ 2.20                 |
|                                   |            | bit=3       | 53.90 | 50.67    | 53.02   | 55.19     | 53.43    | 49.29     | 50.52   | 53.50      | 51.76 | 52.31            | 52.36 $\pm$ 1.80                 |
|                                   |            | bit=5       | 52.45 | 49.93    | 53.51   | 54.38     | 52.64    | 48.46     | 48.95   | 53.55      | 50.36 | 51.53            | 51.58 $\pm$ 2.06                 |
|                                   | Individual | bit=1       | 47.20 | 36.69    | 45.09   | 33.80     | 39.05    | 32.58     | 35.05   | 32.69      | 31.83 | 32.41            | 36.64 $\pm$ 5.50                 |
|                                   |            | bit=3       | 47.29 | 38.19    | 45.65   | 35.63     | 40.70    | 34.27     | 34.31   | 32.29      | 32.73 | 33.38            | 37.44 $\pm$ 5.42                 |
|                                   |            | bit=5       | 45.71 | 37.30    | 44.29   | 34.57     | 39.18    | 33.20     | 33.69   | 32.82      | 31.68 | 32.99            | 36.54 $\pm$ 5.00                 |
| ADG<br>(Zhang et al., 2021)       | Whole      | 48.91       | 46.14 | 48.99    | 50.08   | 49.39     | 44.54    | 44.34     | 49.59   | 45.20      | 48.35 | 47.55 $\pm$ 2.25 |                                  |
|                                   | Individual | 42.95       | 41.15 | 44.05    | 37.09   | 45.07     | 35.89    | 36.99     | 36.35   | 33.69      | 35.39 | 38.86 $\pm$ 4.06 |                                  |
| PLMmark (Li et al., 2023b)        |            |             | 42.39 | 42.43    | 43.96   | 42.73     | 43.92    | 43.79     | 44.07   | 43.69      | 44.81 | 43.23            | 43.50 $\pm$ 0.79                 |
| Ours                              | 7B         | $\alpha=2$  | 57.69 | 65.31    | 52.01   | 65.89     | 64.72    | 59.81     | 56.33   | 60.70      | 61.02 | 63.20            | 60.67 $\pm$ 4.41                 |
|                                   |            | $\alpha=4$  | 60.00 | 69.08    | 55.62   | 67.31     | 65.06    | 61.53     | 57.40   | 62.14      | 60.88 | 62.06            | 62.11 $\pm$ 4.15                 |
|                                   |            | $\alpha=8$  | 62.58 | 70.66    | 55.91   | 69.65     | 67.92    | 65.88     | 66.66   | 65.43      | 67.01 | 65.93            | <b>65.76<math>\pm</math>4.13</b> |
|                                   |            | $\alpha=16$ | 59.99 | 69.49    | 55.68   | 67.85     | 66.47    | 66.35     | 66.39   | 63.48      | 66.89 | 66.22            | 64.88 $\pm$ 4.13                 |
|                                   |            | $\alpha=32$ | 58.50 | 69.64    | 55.73   | 69.08     | 68.39    | 66.95     | 67.39   | 64.08      | 66.22 | 66.26            | 65.22 $\pm$ 4.61                 |
|                                   | 13B        | $\alpha=48$ | 58.92 | 69.60    | 54.42   | 68.61     | 66.89    | 67.03     | 67.51   | 65.33      | 67.38 | 66.77            | 65.25 $\pm$ 4.78                 |
|                                   |            | $\alpha=32$ | 60.50 | 65.18    | 56.60   | 65.25     | 59.72    | 65.53     | 61.78   | 58.99      | 62.11 | 60.97            | 61.66 $\pm$ 2.96                 |